

# Electron Transport in the Long-Range Charge-Recombination Dynamics of Single Encapsulated Dye Molecules on TiO<sub>2</sub> Nanoparticle Films\*\*

Xiangyang Wu, Toby D. M. Bell, and Edwin K. L. Yeow\*

Interfacial electron transfer in dye-sensitized semiconductors, such as TiO<sub>2</sub>, has been applied extensively in molecular devices for solar energy conversion. Electron transport in nanocrystalline metal oxides is an important process that is often neglected when describing the charge-recombination dynamics between injected electrons and TiO<sub>2</sub> at the single-molecule level.<sup>[1,2]</sup> Electron transport is intrinsic to TiO<sub>2</sub> and has been reported to take place on solid-state colloidal TiO<sub>2</sub> films<sup>[3]</sup> and TiO<sub>2</sub> films filled with electrolytes.<sup>[4]</sup> It has been proposed that electron transport occurs by a series of charge trapping and detrapping steps, with the trap sites located predominantly on the metal oxide surface.<sup>[5]</sup> Herein, we examine the role of electron transport in determining the charge-recombination dynamics between single dye molecules and TiO<sub>2</sub>.

One of the major drawbacks of molecular devices is the photodegradation of the dyes used. Supramolecular dyes formed by the encapsulation of dye molecules by macrocyclic hosts, such as cucurbit[7]uril, are known to be highly thermally stable and photostable.<sup>[6]</sup> Cucurbit[7]uril (CB7; Scheme 1) effectively complexes rhodamine 6G (R6G); the significant

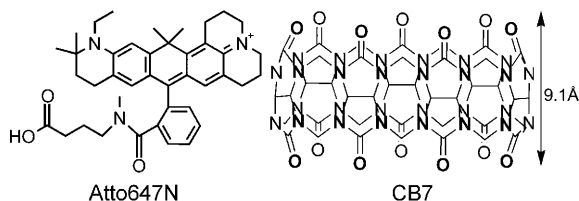
increase in the photostability of R6G upon CB7 encapsulation has been demonstrated at both the bulk and single-molecule levels.<sup>[7,8]</sup> Furthermore, it is advantageous to study the effects of CB7 on the charge-recombination of single dye molecules. Herein, Atto647N, a rhodamine-type dye (Scheme 1) is used to photosensitize TiO<sub>2</sub> nanoparticles. The binding equilibrium constant of the inclusion complex CB7–Atto647N was determined to be 2290 from UV/Vis measurements (see the Supporting Information).

The ensemble-averaged fluorescence spectrum of Atto647N is significantly quenched when adsorbed onto TiO<sub>2</sub> nanoparticles in water (see the Supporting Information). This is due to an ultrafast electron-transfer process from the dye to TiO<sub>2</sub>, which occurs much faster than the resolution of our time-correlated single-photon counting spectrometer (resolution: ca. 100 ps). The free-energy change  $\Delta G^\circ$  for electron transfer is  $-0.46$  V, which indicates an energetically favorable electron-transfer process from the dye to TiO<sub>2</sub> (see the Supporting Information).

Two distinct groups of blinking behavior are observed from the emission intensity time traces of 240 Atto647N molecules on TiO<sub>2</sub> (Figure 1). Of these 240 molecules, 197 (or 82 %) displayed temporary off-events that last from tens of milliseconds to a few seconds (see Figure 1a for a typical trace), whilst the rest of the molecules showed constant emission intensity (that is, absence of blinking) before undergoing irreversible photobleaching. The off-events are attributed to the dark oxidized states of Atto647N formed as a result of interfacial electron transfer from the dye molecule to TiO<sub>2</sub> nanoparticle. The transition from “off” to “on” states occurs when the electron injected into the conduction band of TiO<sub>2</sub> recombines with the oxidized dye to form the fluorescent molecule.

A number-density analysis was performed, which showed that the majority of the Atto647N molecules deposited on TiO<sub>2</sub> were probed in the single-molecule experiment (see the Supporting Information). Furthermore, the fluorescence lifetime ( $\tau_f$ ) distribution of single Atto647N on TiO<sub>2</sub> was fitted to a Gaussian distribution with a mean value of 3.9 ns, which is close to the ensemble-averaged emission lifetime of Atto647N in water (ca. 3.6 ns; see the Supporting Information).

In general, ensemble-averaged forward electron-transfer (FET) rates, which were measured by bulk techniques, fall in the ultrafast time domain (that is, fs to ps), and they are much faster than the resolution of the single-molecule experimental set-up.<sup>[10]</sup> The observation of fluorescence intensity of single dye molecules undergoing rapid electron transfer to metal



**Scheme 1.** Atto647N<sup>[9]</sup> and cucurbit[7]uril (CB7). The depth of CB7 is 9.1 Å.<sup>[16]</sup>

[\*] X. Wu, Prof. Dr. E. K. L. Yeow  
Division of Chemistry and Biological Chemistry, School of Physical and Mathematical Sciences, Nanyang Technological University  
Singapore 637371 (Singapore)  
Fax: (+65) 6791-1961  
E-mail: edwinyeow@ntu.edu.sg  
Homepage: <http://www3.ntu.edu.sg/home/edwinyeow/website/>  
Dr. T. D. M. Bell  
School of Chemistry, University of Melbourne  
Parkville 3010, (Australia)

[\*\*] Financial support for this work is provided by the Singapore Ministry of Education ACRF Tier 1 Grant (RG57/06 and RG165/06). T.D.M.B. thanks the University of Melbourne for a Centenary Research Fellowship and FABLS for financial support. The authors thank Wei Wei Yao and Dr. Richard Webster for assistance with the electrochemistry experiments.

Supporting information for this article is available on the WWW under <http://dx.doi.org/10.1002/anie.200902596>.

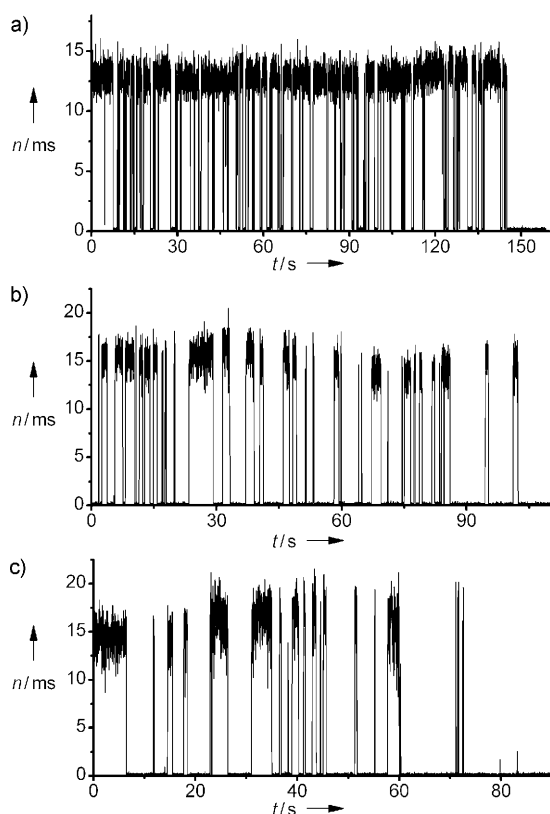


**Figure 1.** Fluorescence intensity time traces (bin time = 20 ms) of single Atto647N (a) and CB7–Atto647N (b,c) molecules on a TiO<sub>2</sub> surface under ambient conditions. *n* is the emission intensity.

oxides was explained by Lu et al., who reported similar behavior in the interfacial electron-transfer dynamics of single dye molecules (such as cresyl violet, coumarin, and porphyrin) on TiO<sub>2</sub>.<sup>[2]</sup> They proposed that the emission intensity of single molecules, such as that seen in Figure 1a, is determined by the fraction of time that the FET process dominates the fluorescence, and it is not affected by the rate of the ultrafast FET. In this case, when the reactivity of FET is low (that is, when FET rate is smaller than the radiative rate), the fluorescence quantum yield and fluorescence intensity are high owing to radiative emission from the excited S<sub>1</sub> state of the dye to its ground state (“on” state and unquenched  $\tau_f$ ). The FET then switches to a high reactivity mode (such as when the FET rate is larger than the radiative rate), which leads to electron transfer to TiO<sub>2</sub> followed by a low or zero fluorescence intensity (“off” state). Several factors, such as the dynamic change of the energy gap between dye and TiO<sub>2</sub>, electronic coupling between the active species, and the vibrational relaxation energy of the adsorbed dye, have been proposed to be responsible for the changing FET reactivities.<sup>[2]</sup>

An off-time ( $\tau_{\text{off}}$ ) duration histogram was constructed using the threshold method.<sup>[11]</sup> The linear log–log plot for the combination of blinking Atto647N molecules on TiO<sub>2</sub> nanoparticle (Figure 2) is best described using a power-law distribution [Eq. (1)]:

$$P(\tau_{\text{off}}) = P_0 \tau_{\text{off}}^{-m_{\text{off}}} \quad (1)$$

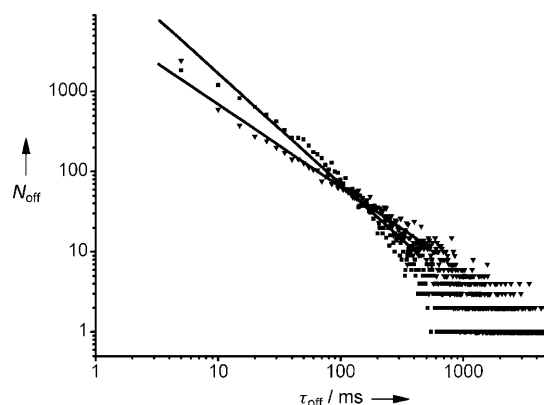
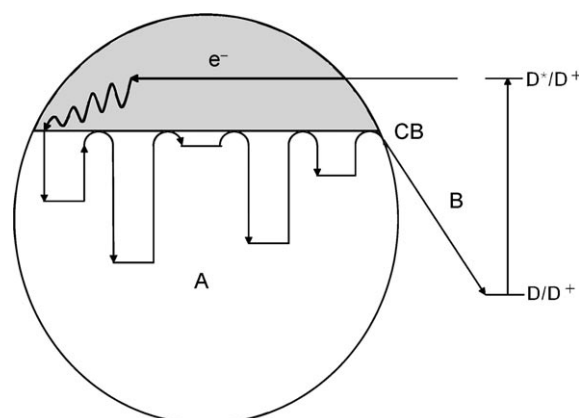


**Figure 2.** Off-time distributions for a combination of 197 Atto647N (■) and 478 CB7–Atto647N (▼) molecules on TiO<sub>2</sub> nanoparticle film. The linear log–log plots yield  $m_{\text{off}}$  values of 1.4 for Atto647N and 1.0 for CB7–Atto647N.  $N_{\text{off}}$  is the number of off-time events and  $\tau_{\text{off}}$  is the off-time.

with the power-law exponent  $m_{\text{off}} = 1.4$ . On the other hand, the on-time histograms do not show a monoexponential decay, thus indicating that the conversion rate from low to high activity does not assume a fixed value (see the Supporting Information).

Following electron injection into the TiO<sub>2</sub> conduction band and fast relaxation, the injected electron undergoes electron transport by moving from trap to trap on the TiO<sub>2</sub> surface by a series of trapping and thermally activated detrapping events. Thereafter, the electron arrives at a suitable reactive site, where it undergoes interfacial back electron transfer (BET) to the oxidized dye (Scheme 2).<sup>[12]</sup> The classical Marcus equation is commonly used to describe the BET rate  $k_{\text{bet}}$ .<sup>[13]</sup> In Figure 1a, the duration of each off-event ( $\tau_{\text{off}}$ ) is equivalent to the total time for electron transport and interfacial BET. As the dye molecules are in direct contact with the TiO<sub>2</sub> nanoparticles, it is assumed that  $k_{\text{bet}}$  is much faster than the electron detrapping rates at the reactive sites.<sup>[12]</sup> In such a case,  $\tau_{\text{off}}$  is given by the time taken for the injected electron to visit the traps before arriving at a



**Scheme 2.** Electron injection and charge recombination. Following electron injection into the conduction band (CB) and fast relaxation, the injected electron undergoes electron transport (A) and then electron transfer (B) back to the oxidized dye.<sup>[12]</sup>

reactive site (that is, the first passage time). A power-law distribution for the detrapping times of an electron at a trap site,  $P(t) = Pt^{-1-\alpha}$ , where  $0 < \alpha < 1$ , is obtained when an exponential distribution of trap energies  $E_i$  (depicting the Urbach tail in the conduction band edge) is considered [Eq. (2)].<sup>[14]</sup>

$$g(E_i) = \frac{1}{k_B T_0} e^{-(E_c - E_i)/k_B T_0} \quad (2)$$

where  $k_B$  is the Boltzmann's constant and  $E_c$  is the conduction band-edge energy. The characteristic temperature  $T_0$ , the temperature  $T$ , and  $\alpha$  are related by  $\alpha = T/T_0$ . The duration of each off-event is thus the sum of several power-law variables, and follows a power-law distribution with  $m_{\text{off}} = 1 + \alpha$ . Values for  $\alpha$  of circa 0.4 were reported for ruthenium-based dye-sensitized TiO<sub>2</sub> using transient absorption spectroscopy, and these values are in good agreement with the  $\alpha$  value obtained from the off-time distribution (Figure 2).<sup>[14,15]</sup>

The emission intensity time traces of 749 CB7–Atto647N molecules on TiO<sub>2</sub> were recorded and their blinking behavior categorized into two groups. 120 molecules (16%) did not show any blinking behavior, whereas the other 629 molecules showed either long-lived off-events in the fluorescence trajectory (478 molecules, see Figure 1b,c) or rapid “on”/“off” intensity fluctuations with “off” states lasting a few ms (151 molecules). The latter process is due to the dark triplet state of the encapsulated molecule (see the Supporting Information).

The intensity time traces of two typical molecules that exhibit long off-events are illustrated in Figure 1b,c. A power-law distribution for the off-times is observed for the collection of blinking molecules with  $m_{\text{off}} = 1.0$  (Figure 2). The small power-law exponent suggests that there is a higher probability of finding long dark periods when Atto647N molecules are included into CB7 as compared to uncomplexed dyes.

The discrepancy in the observed  $m_{\text{off}}$  values between Atto647N and CB7–Atto647N on TiO<sub>2</sub> is rationalized by considering a reduced rate  $k_{\text{bet}}$  when the dye molecule is included into the macrocyclic CB7. In this case, the electronic coupling matrix element  $H_{\text{el}}$  in  $k_{\text{bet}}$  diminishes exponentially with increasing distance between the electron donating and accepting states  $R_e$ ; the relationship is  $H_{\text{el}}^2 = H_0^2 e^{-\beta R_e}$ , where  $\beta$  is the attenuation factor. When Atto647N is included into CB7, the latter increases the spatial separation between the dye molecule and the metal oxide, thus reducing the value of  $k_{\text{bet}}$  relative to the uncomplexed molecule. In this case, charge recombination is not limited by the first passage time, and the injected electron can visit the reactive sites several times before BET occurs. This results in an increase in the  $\tau_{\text{off}}$  value as observed experimentally.

The above argument is supported by studying the blinking behavior of single CB7–Atto647N molecules surrounded by TiO<sub>2</sub> nanoparticles. In this case, the emission intensity time traces of 240 molecules sandwiched between two layers (top and bottom) of TiO<sub>2</sub> nanoparticle films were recorded. The power-law distribution for the off-time durations, obtained from a combination of 203 blinking molecules, yielded a  $m_{\text{off}}$  value of 1.4, which is similar to the power-law exponent of

uncomplexed Atto647N on TiO<sub>2</sub> nanoparticles. This result means that the probability for faster charge recombination is higher when the oxidized CB7–Atto647N molecule is completely surrounded by TiO<sub>2</sub> nanoparticles than when it is in contact with only a bottom layer of metal oxide. It has been shown that the internal cavity of a CB7 is too small to fully accommodate a R6G molecule by computational chemistry calculations,<sup>[8]</sup> which suggests that the larger Atto647N molecule is partially encapsulated by CB7. For CB7–Atto647N on a bottom layer of TiO<sub>2</sub>, the part of the molecule that is not protected by CB7 is separated from the metal oxide. On the other hand, for CB7–Atto647N surrounded by TiO<sub>2</sub> (that is, by both top and bottom layers), the unprotected part of the dye is in direct contact with the metal oxide, thus enabling interfacial BET to occur without spatial distance effects.

Long off-events may occur when high FET activity persists for a long time.<sup>[2]</sup> The greater spatial separation between CB7–Atto647N and TiO<sub>2</sub> may result in either unchanged or shorter periods of high FET activity compared to the uncomplexed molecule. Clearly, FET activity alone does not completely describe the off-events, and electron transport plays an important role in the observed fluorescence intermittency.

Computational simulations, based on a continuous-time random walk, were performed to obtain off-time distributions (see the Supporting Information for details).<sup>[12]</sup> A probability  $P_{\text{bet}} = k_{\text{bet}}/(v_o + k_{\text{bet}})$  is introduced to decide if the electron at a reactive site recombines or hops to a neighboring trap with rate  $v_o$  (the electron attempt-to-escape frequency). In this case,  $P_{\text{bet}} = 1$  when fast BET is present ( $k_{\text{bet}} \gg v_o$ ), and  $P_{\text{bet}}$  tends to zero for slow BET (when  $v_o \gg k_{\text{bet}}$ ). A value  $v_o = 1 \times 10^{10} \text{ s}^{-1}$  that is smaller than the atomic frequency (ca.  $10^{12} \text{ s}^{-1}$ ) is utilized in the simulation. Figure 3 shows the normalized off-time distributions for various  $P_{\text{bet}}$  values obtained from computational simulations. The off-times follow a power-law distribution with  $m_{\text{off}} = 1.4$  ( $\alpha = 0.4$ ), 1.3 ( $\alpha = 0.3$ ), 1.1 ( $\alpha = 0.1$ ) and 1.0 ( $\alpha = 0$ ) for  $P_{\text{bet}} = 1$ , 0.01, 0.001, and 0.0005, respectively. When an electron at a reactive site has an increased probability of hopping to a trap, the charge-

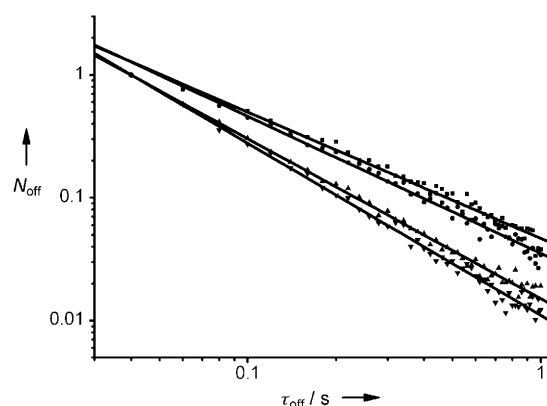


**Figure 3.** Normalized off-time distributions based on the Monte Carlo simulations. The linear log–log plots yield  $m_{\text{off}}$  values of 1.4 ( $P_{\text{bet}} = 1$ ,  $\blacktriangledown$ ), 1.3 (0.01,  $\blacktriangle$ ), 1.1 (0.001,  $\bullet$ ), and 1.0 (0.0005,  $\blacksquare$ ).  $N_{\text{off}}$  is the number of off-time events and  $\tau_{\text{off}}$  is the off-time.

recombination dynamics is no longer limited by the first-passage time. The electron continues to diffuse on the metal oxide surface, and undergoes several encounters with the reactive site before BET occurs. This results in an increase in the probability of finding long off-times, and a concomitant decrease in the  $\alpha$  value in accordance with experimental observation. Similar trends are observed when different  $v_o$  values are employed in the simulations.

The configuration with the empty portal of CB7 sitting on the nanoparticle will result in a maximum separation between the unprotected portion of the dye and  $\text{TiO}_2$  and gives rise to long off-events. In this case, the separation between the unprotected dye and the metal oxide is at least the depth of the macrocyclic CB7 (ca. 9 Å).<sup>[16]</sup> This is the most important configuration for the long off-events. When  $m_{\text{off}} = 1.0$ ,  $v_o = 1 \times 10^{10} \text{ s}^{-1}$  and  $P_{\text{bet}} = 0.0005$ , a value of  $k_{\text{bet}} \approx 5 \times 10^6 \text{ s}^{-1}$  is obtained for the back electron-transfer reaction between the inclusion complex and  $\text{TiO}_2$ . The exact separation  $R_e$  between Atto647N and  $\text{TiO}_2$  is not known, and by assuming an  $R_e$  value of 9 Å (the depth of CB7) and an attenuation factor of  $\beta = 1 \text{ Å}^{-1}$ ,<sup>[12]</sup> a value of  $k_{\text{bet}} \approx 4 \times 10^{10} \text{ s}^{-1}$  is obtained for the uncomplexed dye. This value is reasonable, as several studies have shown that interfacial BET occurs within a few ps to ns.<sup>[17]</sup>

In summary, we have detected the presence of long-lived dye cations in the majority of dye molecules on  $\text{TiO}_2$ , and especially for the encapsulated Atto647N, and have demonstrated that electron transport may play a pivotal role in charge recombination at the single-molecule level, as it adequately describes the power-law dispersion of  $\tau_{\text{off}}$ .

Received: May 15, 2009

Revised: July 7, 2009

Published online: September 1, 2009

**Keywords:** charge recombination · electron transport · single-molecule spectroscopy · titanium dioxide

- [1] a) M. W. Holman, R. Liu, D. M. Adams, *J. Am. Chem. Soc.* **2003**, *125*, 12649–12654; b) H. P. Lu, X. S. Xie, *J. Phys. Chem. B* **1997**,

- 101*, 2753–2757; c) T. D. M. Bell, C. Pagba, M. Myahkostupov, J. Hofkens, P. Piotrowiak, *J. Phys. Chem. B* **2006**, *110*, 25314–25321; d) T. Tachikawa, S. Ciu, S. Tojo, M. Fujitsuka, T. Majima, *Chem. Phys. Lett.* **2007**, *443*, 313–318.  
[2] a) V. Biju, M. Miodrag, D. Hu, H. P. Lu, *J. Am. Chem. Soc.* **2004**, *126*, 9374–9381; b) Y. Wang, X. Wang, S. K. Ghosh, H. P. Lu, *J. Am. Chem. Soc.* **2009**, *131*, 1479–1487.  
[3] R. Könenkamp, R. Henninger, P. Hoyer, *J. Phys. Chem.* **1993**, *97*, 7328–7330.  
[4] R. Katoh, A. Furube, A. V. Barzykin, H. Arakawa, M. Tachiya, *Coord. Chem. Rev.* **2004**, *248*, 1195–1213.  
[5] N. Kopidakis, N. R. Neale, K. Zhu, J. van de Lagemaat, A. J. Frank, *Appl. Phys. Lett.* **2005**, *87*, 202106.  
[6] A. L. Koner, W. N. Nau, *Supramol. Chem.* **2007**, *19*, 55–66.  
[7] J. Mohanty, W. N. Nau, *Angew. Chem.* **2005**, *117*, 3816–3820; *Angew. Chem. Int. Ed.* **2005**, *44*, 3750–3754.  
[8] T. A. Martyn, J. L. Moore, R. L. Halterman, W. T. Yip, *J. Am. Chem. Soc.* **2007**, *129*, 10338–10339.  
[9] C. Eggeling, C. Ringemann, R. Medda, G. Schwarzmann, K. Sandhoff, S. Polyakova, V. N. Belov, B. Hein, C. von Middendorff, A. Schönle, S. W. Hell, *Nature* **2009**, *457*, 1159–1163.  
[10] a) D. F. Watson, G. J. Meyer, *Annu. Rev. Phys. Chem.* **2005**, *56*, 119–156; b) N. A. Anderson, T. Lian, *Annu. Rev. Phys. Chem.* **2005**, *56*, 491–519.  
[11] a) E. K. L. Yeow, S. M. Melnikov, T. D. M. Bell, F. C. De Schryver, J. Hofkens, *J. Phys. Chem. A* **2006**, *110*, 1726–1734; b) X. Wu, E. K. L. Yeow, *Nanotechnology* **2008**, *19*, 035706.  
[12] J. N. Clifford, E. Palomares, M. K. Nazeeruddin, M. Grätzel, J. Nelson, X. Li, N. J. Long, J. R. Durrant, *J. Am. Chem. Soc.* **2004**, *126*, 5225–5233.  
[13] R. A. Marcus, N. Sutin, *Biochim. Biophys. Acta* **1985**, *811*, 265–322.  
[14] a) J. Nelson, *Phys. Rev. B* **1999**, *59*, 15374–15380; b) J. Nelson, S. A. Haque, D. R. Klug, J. R. Durrant, *Phys. Rev. B* **2001**, *63*, 205321; c) J. Nelson, R. E. Chandler, *Coord. Chem. Rev.* **2004**, *248*, 1181–1194.  
[15] S. A. Haque, Y. Tachibana, R. L. Willis, J. E. Moser, M. Grätzel, D. R. Klug, J. R. Durrant, *J. Phys. Chem. B* **2000**, *104*, 538–547.  
[16] J. Lagona, P. Mukhopadhyay, S. Chakrabarti, L. Isaacs, *Angew. Chem.* **2005**, *117*, 4922–4949; *Angew. Chem. Int. Ed.* **2005**, *44*, 4844–4870.  
[17] a) Y. Weng, Y. Wang, J. B. Asbury, H. N. Ghosh, T. Lian, *J. Phys. Chem. B* **2000**, *104*, 93–104; b) G. Ramakrishna, H. N. Ghosh, A. K. Singh, D. K. Palit, J. P. Mittal, *J. Phys. Chem. B* **2001**, *105*, 12786–12796.